

Research Article

Optimizing NMR fragment-based drug screening for membrane protein targets

Geoffrey C. Li¹, Manuel A. Castro¹, Thilini Ukwaththage, Charles R. Sanders*

Department of Biochemistry and Center for Structural Biology, Vanderbilt University School of Medicine – Basic Sciences, Nashville, TN 37240, USA



ARTICLE INFO

Keywords:

NMR spectroscopy
 Fragment-based drug discovery
 FBDD
 Fragment-based screening
 Membrane protein
 Protein-small molecule interactions
 C99
 PMP22
 Peripheral myelin protein 22
 Amyloid precursor protein

ABSTRACT

NMR spectroscopy has played a pivotal role in fragment-based drug discovery by coupling detection of weak ligand-target binding with structural mapping of the binding site. Fragment-based screening by NMR has been successfully applied to many soluble protein targets, but only to a limited number of membrane proteins, despite the fact that many drug targets are membrane proteins. This is partly because of difficulties preparing membrane proteins for NMR—especially human membrane proteins—and because of the inherent complexity associated with solution NMR spectroscopy on membrane protein samples, which require the inclusion of membrane-mimetic agents such as micelles, nanodiscs, or bicelles. Here, we developed a generalizable protocol for fragment-based screening of membrane proteins using NMR. We employed two human membrane protein targets, both in fully protonated detergent micelles: the single-pass C-terminal domain of the amyloid precursor protein, C99, and the tetraspan peripheral myelin protein 22 (PMP22). For both we determined the optimal NMR acquisition parameters, protein concentration, protein-to-micelle ratio, and upper limit to the concentration of D₆-DMSO in screening samples. Furthermore, we conducted preliminary screens of a plate-format molecular fragment mixture library using our optimized conditions and were able to identify hit compounds that selectively bound to the respective target proteins. It is hoped that the approaches presented here will be useful in complementing existing methods for discovering lead compounds that target membrane proteins.

Introduction

Fragment based drug discovery (FBDD) has been a powerful technique for use in the development of lead compounds in early stage drug discovery. (Erlanson et al., 2016; Murray and Rees, 2009; Rees et al., 2004; Carr et al., 2005; Hajduk and Greer, 2007) As opposed to conventional high throughput screening, fragment-based screening uses a library of low molecular weight compounds, referred to as “fragments” (MW ≤ 300 Da), in a search for ligands that bind to the target, usually with low affinity. Due to the small size of the fragments and their diverse functional groups, this approach offers the advantage of providing a facile route to sampling a wide range of chemical space, followed by facile purchase or synthesis of analogs of the parent fragment to probe structure–activity relationships (SAR). In an ideal case, two or more SAR-optimized fragments that bind to adjacent sites can then be chemically linked to yield drug-like bidentate compounds that exhibit partially additive binding energies (Murray et al., 2012; Erlanson and Hansen, 2004).

Due to the weak affinities of the fragments, NMR spectroscopy is a particularly suitable biophysical techniques for detecting and characterizing binding, including determination of the dissociation constant (K_d). The lab of Stephen Fesik first introduced FBDD in which they used NMR spectroscopy to develop a high-affinity ligand to the FK506 binding protein. Their approach was dubbed “SAR by NMR”. (Shuker et al., 1996) Since then, multiple variations of NMR-based approaches have been developed and employed in FBDD. (Fejzo et al., 2003; Homans, 2004; Mureddu and Vuister, 2022; Fesik et al., 1997) These include ligand-observed methods where changes in the spectra of ligands are monitored, such as saturation transfer difference (STD) (Mayer and Meyer, 1999; Mayer and Meyer, 2001; Viegas et al., 2011); WaterLOGSY (Dalvit et al., 2000; Dalvit et al., 2001), and ¹⁹F NMR. (Dalvit et al., 2002; Jordan et al., 2012; Teng et al., 2004; Norton et al., 2016; Buchholz and Pomerantz, 2021) However, the most commonly used methods involve monitoring changes in the NMR spectrum of the protein as the fragment is titrated in, most often in the form of a series of 2D ¹⁵N-HSQC spectra (Shuker et al., 1996; Hajduk et al., 1999; Hajduk

* Corresponding author.

E-mail address: chuck.sanders@vanderbilt.edu (C.R. Sanders).¹ These authors contributed equally.

et al., 1999).

Applying NMR-based FBDD to membrane proteins poses a challenge, in part because membrane proteins require high concentrations of membrane mimetics containing detergents and/or lipids to maintain target solubility and stability. The strong signals coming from the protons of these membrane mimetics sometimes interfere with the detection of protons from either the protein or the fragments. Moreover, the fragments typically used in screening are often hydrophobic enough to preferentially partition into the membrane-mimetic phase, complicating the analysis of 1D ^1H spectra from the ligand, sometimes leading to false positive or false negative results. In addition to these technical challenges, membrane proteins typically have relatively low yields when expressed recombinantly in bacterial systems, which may be a serious hindrance, particularly for screens requiring hundreds of samples. These considerations help explain why there have only been a few reported NMR-based fragment-based screens carried out with membrane protein targets. Approaches undertaken to circumvent these challenges include target-immobilized NMR screening (TINS) (Vanwetswinkel et al., 2005), where the target is immobilized on a solid support and a fragment mixture is applied, with binding being detected by comparing the 1D ^1H NMR spectra of the fragments in the eluate for target versus reference (control) samples. This method was successfully applied to a G-protein coupled receptor (GPCR) (Congreve et al., 2011; Chen et al., 2012) and to DsbB. (Fruh et al., 2010) Applications of STD NMR to membrane protein fragment screening have been demonstrated with integrin $\alpha_{\text{IIb}}\beta_3$ that is embedded in a liposome (Meinecke and Meyer, 2001), or with a stabilized GPCR (Igonet et al., 2018). Alternatively, investigators have used heteronuclear NMR for detection of the fragments. For example, ^{19}F NMR has previously been applied in screening of a membrane-bound enzyme, fatty acid amide hydrolase, using a fluorinated fragment library (Tengel et al., 2004; Lambruschini et al., 2013).

Protein-detected 2D $^1\text{H},^{15}\text{N}$ -HSQC FBDD screening approaches remain by far the most commonly used method in fragment-based screening and leads to fewer false positives than most other methods. With this approach, one can also screen mixtures of fragments to optimize throughput. Furthermore, if the target's backbone amide $^1\text{H},^{15}\text{N}$ resonances are assigned this approach allows one to map out the site of ligand interaction. (Shuker et al., 1996; Hajduk et al., 1999; Hajduk et al., 1999) Another virtue of this approach is that with judicious choice of the exact HSQC pulse sequence, it is possible to filter out signals from all protons in the sample that are not directly attached to an ^{15}N atom, allowing the elimination of spectral interference from even very high concentrations of fully protonated membrane mimetic compounds (e.g. detergents). For larger proteins and for sizable membrane protein-membrane mimetic complexes, the TROSY pulse program can be employed instead of HSQC in order to obtain HSQC-like spectra, but with more narrow contour peak linewidths and resulting better-resolved spectra.

In this paper, we developed NMR-based fragment screening protocols for two human membrane protein targets: (i) the single pass C99 protein that is the immediate precursor of the amyloid beta ($\text{A}\beta$) polypeptides (Castro et al., 2019; Chow et al., 2010) closely associated with Alzheimer's disease, and (ii) the tetraspan membrane protein peripheral myelin protein 22 (PMP22), a key component of the myelin sheath in the peripheral nervous system and subject to genetic variations that cause Charcot-Marie-Tooth disease. (Jetten and Suter, 2000) This required customization of the FBDD approach for these proteins. We first optimized the membrane protein screening conditions, including choice of NMR pulse program, protein concentration, protein-to-micelle ratio, and maximum allowable amount of added D_6 -DMSO vehicle. We then used these optimized conditions to screen mixtures of molecular fragments, followed by identification and characterization of the hits that bind selectively to the target proteins. This work offers case studies that provide a roadmap for conducting NMR-based fragment screening of membrane proteins. The scope of this work is that we are only focusing on the critical first steps (sample preparation and fragment screening) of

FBDD.

Results

Choice of membrane protein targets

Our screening effort focused on two disease-related human membrane protein targets: (i) C99, the 99-residue single pass transmembrane C-terminal domain of the amyloid precursor protein, and (ii) peripheral myelin protein 22, a 160-residue tetraspan protein found in the myelin sheath of the peripheral nerves: PMP22. (Jetten and Suter, 2000) Cleavage of C99 by γ -secretase releases the $\text{A}\beta$ peptides that are associated with Alzheimer's disease. (Castro et al., 2019; Chow et al., 2010) Genetic aberrations of PMP22 cause the most common forms of the peripheral neuropathy Charcot-Marie-Tooth disease. (Li et al., 2013) The structure of C99 was previously determined by NMR in lysomyristoylphosphatidylglycerol (LMPG) micelles (Barrett et al., 2012), whereas PMP22 yields only medium quality NMR spectra, with dodecyl- β -maltopyranoside (DDM) micelles yielding the highest quality spectra among many different micelle and bicelle conditions tested. (Stefanski et al., 2023) We first optimized sample conditions and NMR parameters for use in HTS for molecular fragments that bind to these proteins.

C99, a single pass transmembrane protein

- Pulse Program.** High throughput screening pipelines require collection of high-quality spectra with a minimal data acquisition time. We tested several 2D $^1\text{H},^{15}\text{N}$ NMR experiments at identical total experiment times to evaluate which would yield the highest quality NMR spectrum of C99. The tested pulse programs (Bruker-coded) were SOFAST-HMQC (Schanda et al., 2005) (sfhmqcf3gpph), two versions of BEST-TROSY (Favier and Brutscher, 2011) (b_trosyef3gpsi.3 and b_trosyf3gpph.2), and a clean TROSY-HSQC (Per-vushin et al., 1997; Schulte-Herbruggen and Sorensen, 2000) pulse program (trosyef3gpsi.2) (Fig. 1) at 600 MHz. For details of the NMR pulse programs, see Materials and Methods. Using a total experiment time of 30 min and a 3 mm sample with C99 concentrations of 50, 150, and 450 μM , the clean TROSY-HSQC provided a disappointing NMR spectrum with only low signal-to-noise ratios and a number of missing resonances. The SOFAST-HMQC gave the highest signal-to-noise ratios; however, the spectral resolution was sub-optimal due to broader linewidths, resulting in significant peak overlap. One of the BEST-TROSY programs, b_trosyf3gpph.2, was seen to represent a happy medium between optimal signal-to-noise and spectral resolution. We used this pulse program moving forward.
- Protein Concentration.** For NMR-based screening requiring numerous samples, the amount of available membrane protein is almost always a limiting factor. To efficiently screen thousands of compounds, it is imperative to obtain decent quality NMR spectra with the least amount of protein possible. We tested three different concentrations of C99 (50, 150, and 450 μM) at 20 % (w/v) LMPG. For 30-minute BEST-TROSY experiments at 600 MHz it was possible to secure satisfactory NMR spectra even for 50 μM C99 (Fig. 1). With 200 μL 3 mm NMR samples of 50 μM C99, it was possible to screen an entire 96-well plate of molecular fragment mixtures (12 fragments in each well) using the protein purified from 12 L of *E. coli* culture grown in M9 minimal media. In all our experiments, we chose a salt concentration of 100 mM to simulate the physiological salt concentration, at the expense of some reduction in single-to-noise due to lossiness.
- Protein-to-Micelle Ratio.** The protein-to-micelle ratio is an important consideration when studying membrane proteins in detergent micelles. (Opella et al., 1994) A 1:1 or otherwise high protein-to-micelle ratio may cause the co-habitation of multiple membrane proteins in one detergent micelle (Zhuang et al., 2011), which may promote aggregation or non-specific homo-oligomerization. Also,

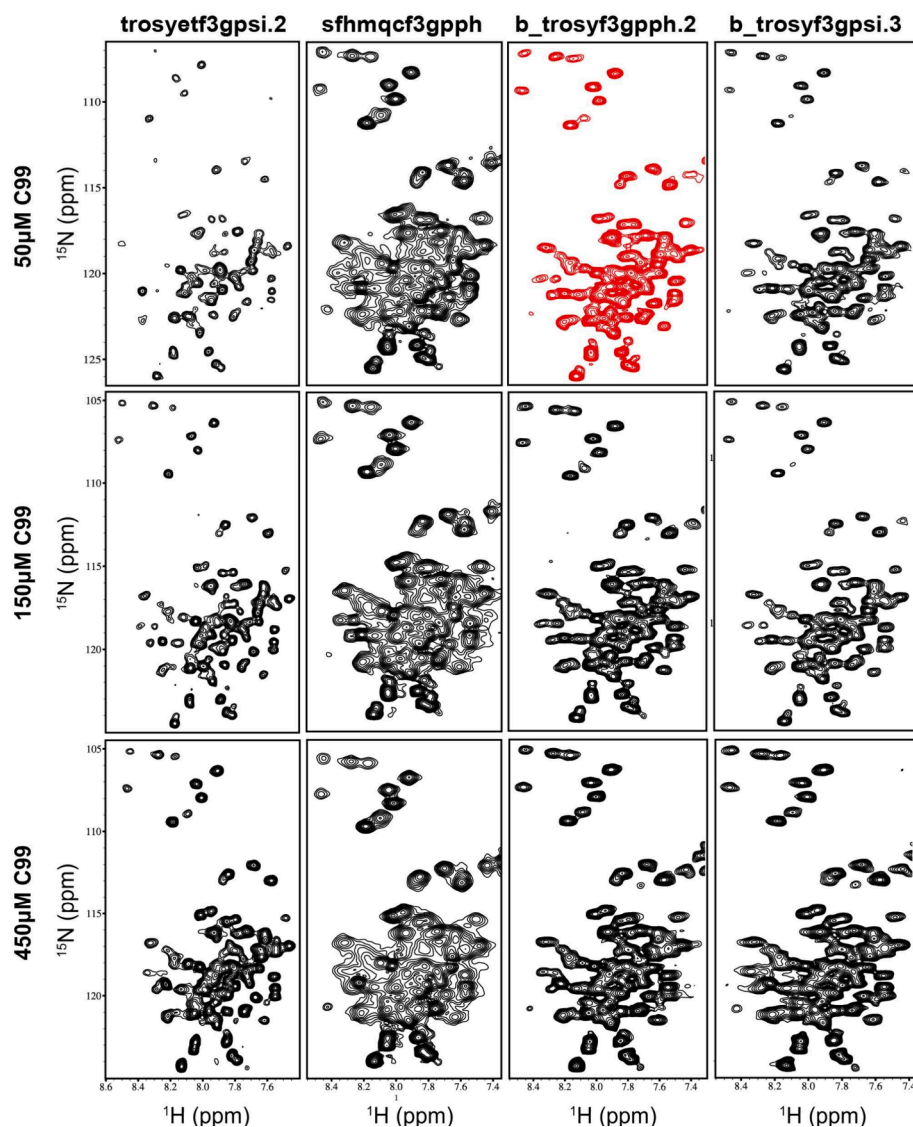


Fig. 1. Pulse program optimization for C99 screening. Shown here are spectra for uniformly ^{15}N -labelled C99 spectra in LMPG using four different pulse programs and three different protein concentrations. At the 50 μM point, the BEST-TROSY-2 (b_trotyf3gpph.2; in red) program yielded the best signal-to-noise and resolution at this protein low concentration. Experiments were acquired at a sample temperature of 45 $^{\circ}\text{C}$ and a field of 600 MHz. Recycle delay = 1.5 s for troyetf3gpsi.2, 0.2 s for sfhmqcf3gpph, b_trotyf3gpph, and b_trotyf3gpsi.3; number of scans = 8 for troyetf3gpsi.2, 64 for sfhmqcf3gpph, b_trotyf3gpph, and b_trotyf3gpsi.3; number of complex data points: (2048, 128) for troyetf3gpsi.2, (1024, 96) for sfhmqcf3gpph, b_trotyf3gpph, and b_trotyf3gpsi.3 in the ^1H and ^{15}N dimensions, respectively; spectral width: 14 ppm in the ^1H and 27 ppm in the ^{15}N dimensions for all four pulse sequences.

because the molecular fragments being screened are generally hydrophobic, even non-binders will often preferentially partition into detergent micelles (relative to the aqueous phase). A too-high protein-to-micelle ratio may force the protein and partitioned compounds to colocalize in the same micelle, promoting false positive results—changes in the NMR spectrum resulting from forced non-specific compound-detergent-protein interactions. Hence, it was imperative to optimize the amount of detergent (in this case, LMPG) to balance NMR spectral quality with the need for sufficiently high concentrations of micelles to select against forced cohabitation. Considering the published LMPG aggregation number of 65 (Oliver et al., 2013), we tested LMPG total concentrations of 0.25 % (w/v) (5.2 mM LMPG; 0.08 mM micelles), 2.5 % (w/v) (52 mM LMPG; 0.8 mM micelles), and 17.5 % (w/v) (364 mM LMPG; 5.6 mM micelles) (Fig. 2). This corresponded to moles of protein-to-micelle ratios of 1:1.6, 1:16, and 1:112, respectively. Something to keep in mind is that membrane proteins can influence the actual aggregation number of micelles they reside in, so these calculated ratios should be

regarded as an approximation. (Vinogradova et al., 1998) NMR spectral quality was relatively poor at 0.25 % LMPG but was significantly improved at 2.5 % and 17.5 %. Since the spectral quality of 2.5 % and 17.5 % LMPG were nearly identical and because we deem that a protein-to-micelle ratio of 1:16 was likely sufficient to avoid forced cohabitation, the 2.5 % LMPG condition was chosen for use in screening.

- 4. D_6 -DMSO Concentration.** The final condition that we optimized is the final concentration in the NMR sample of D_6 -DMSO, which serves as the vehicle used to solubilize test compounds (or mixtures) prior to addition to micellar C99 solutions. We aimed to determine the highest possible D_6 -DMSO concentration that can be present in the micellar NMR sample before the NMR spectrum of C99 became significantly perturbed. We tested D_6 -DMSO concentrations from 0 to 4 % (v/v) at 2.5 % LMPG (Fig. 2). We found that C99 was tolerant to D_6 -DMSO concentration up to 4 %, with only very modest perturbations in the C99 TROSY spectrum. We performed this in triplicate and found that the spectra were reproducible, suggesting

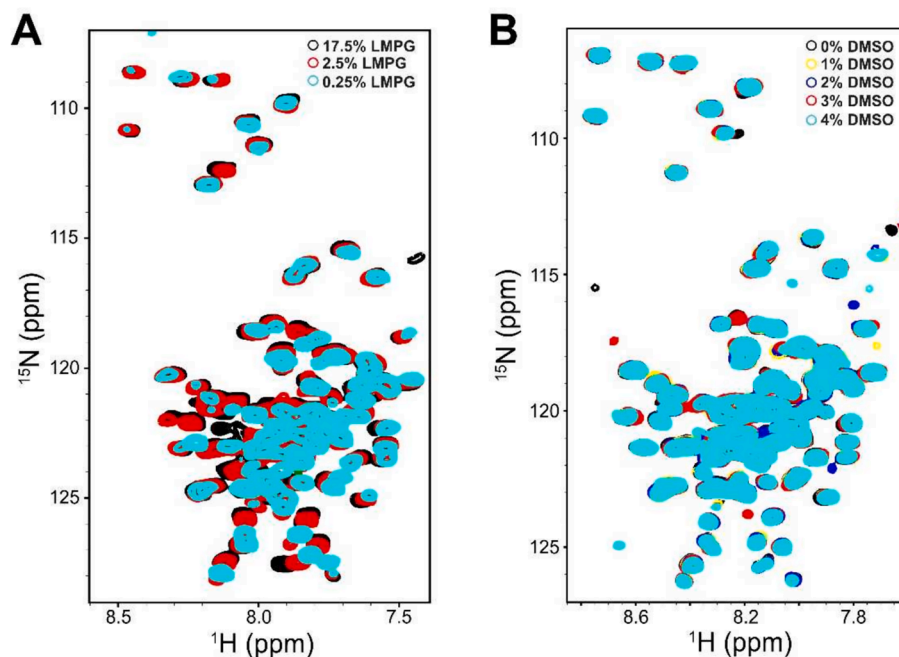


Fig. 2. Optimization of LMPG and D₆-DMSO concentrations for screening C99. A) Three overlaid spectra of ¹⁵N-labeled C99 at different LMPG concentrations. Overall, the C99 spectra looked similar at 2.5 % w/v and 17.5 % w/v concentrations but are of markedly lower quality at the lower 0.25 % w/v point. B) Five overlaid C99 spectra at D₆-DMSO concentrations ranging from 0 % to 4 % v/v. Overall, D₆-DMSO had very little effect on C99 spectral quality, suggesting it was resistant to the ‘D₆-DMSO effect’ at these relatively low concentrations. Experiments were acquired at a sample temperature of 45 °C and a field of 600 MHz. For both (A) and (B), recycle delay = 0.2 s; number of scans = 64, number of complex data points: 1024 in the ¹H and 96 in the ¹⁵N dimensions; spectral width: 14 ppm in the ¹H and 27 ppm in the ¹⁵N dimensions.

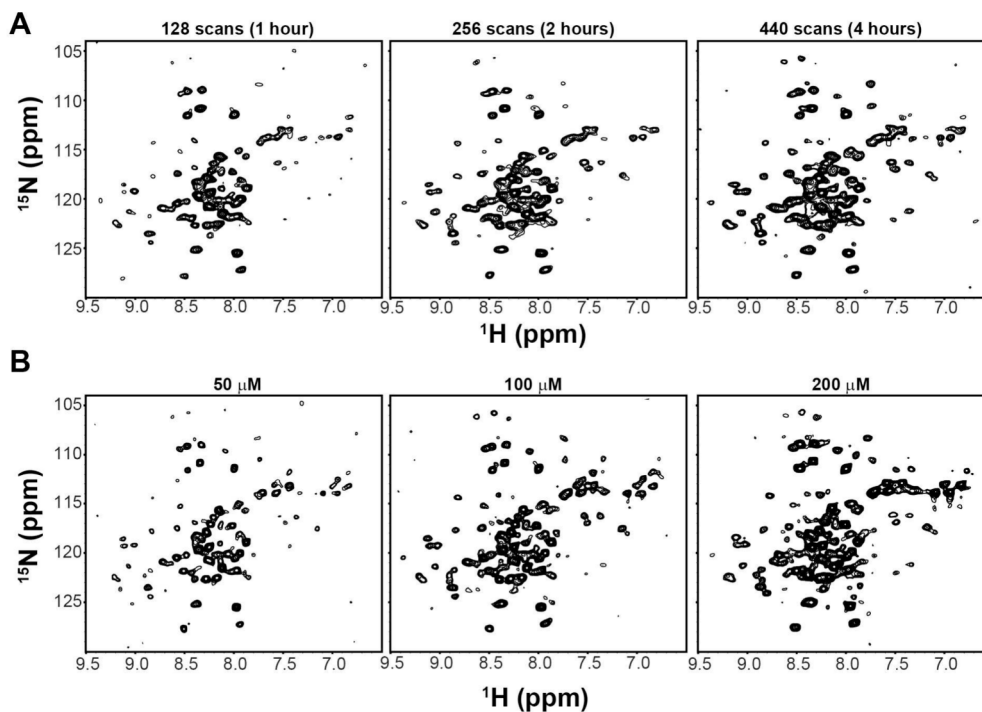


Fig. 3. Optimization of the number of scans and protein concentration for screening PMP22. A) Spectra of PMP22 acquired using the BEST-TROSY (b_rossy3gpph.2) pulse program with different numbers of scans at 45 °C and 900 MHz. The protein concentration is 100 μM and the DDM concentration is ~ 30 mM (protein-to-micelle ratio = 1:3, based on the DDM aggregation number = 100). The approximate total experiment time for each experiment is indicated. Recycle delay = 0.2 s; number of complex data points: 1024 in the ¹H and 96 in the ¹⁵N dimensions; spectral width: 18 ppm in the ¹H and 28 ppm in the ¹⁵N dimensions. B) The spectra of PMP22 at different protein concentrations. The pulse program used was b_rossy3gpph.2 with 440 scans at 45 °C. Recycle delay = 0.2 s; number of complex data points: 2048 in the ¹H and 96 in the ¹⁵N dimensions; spectral width: 18 ppm in the ¹H and 28 ppm in the ¹⁵N dimensions.

that concentrations up to 4 % D₆-DMSO are not a problem in screening.

Overall, the optimized conditions for C99 screening at 600 MHz using 200 μ l samples in 3 mm NMR tubes were found to be: 50 μ M ¹⁵N-labeled C99 in 2.5 % LMPG (1:16 protein-to-micelle ratio), with up to 4 % D₆-DMSO, and using the 2D BEST TROSY pulse program b_trotyf3gpqh.2.

PMP22, a human tetraspan membrane protein

Having optimized the conditions for screening of a single pass transmembrane protein in detergent micelles, we then optimized the parameters for a multispan membrane protein. We used peripheral myelin protein 22 (PMP22) as an example. PMP22 gives an NMR spectrum of moderate quality in DDM micelles at pH 5 and 45 °C, in which roughly 103 of an expected 168 peaks are observed. Tests spanning a period of years of numerous other detergents and bicelles have not yielded spectra of higher quality. Being a tetraspan membrane protein, it is difficult to record a high quality NMR spectrum in 30 min at 600 MHz. We therefore collected data at 900 MHz and optimized the number of scans for the BEST-TROSY pulse program b_trotyf3gpqh.2 using 100 μ M PMP22 in DDM micelles (Fig. 3A). We tested 128, 256, and 440 scans in the direct dimension (while keeping 96 points in the indirect

dimension). We found that 440 scans gave a satisfactory NMR spectrum for a sample containing 100–200 μ M PMP22 in DDM micelles, with a total experiment time of 4 h. While the PMP22 data presented in this study were based on use of pH 5.0 conditions, we also found that it is possible to screen at pH 6.5, where the quality of the TROSY spectrum is decreased only incrementally.

Even at 900 MHz, 50 μ M PMP22 in a 3 mm NMR tube did not give a good NMR spectrum, even with 440 scans (Fig. 3B). The spectral quality improved at 100 μ M, but was much better improved at 150–200 μ M. To optimize the protein-to-micelle ratio (using an aggregation number of 100 for DDM), we tested two samples, each containing 100 μ M PMP22 but with two different DDM concentrations: 30 mM and 100 mM, corresponding to protein-to-micelle ratios of 1:3 and 1:10 respectively. We did not see a significant difference in spectral quality between 1:3 and 1:10; however, we chose 1:10 as the optimal ratio to avoid the forced cohabitation of protein and added fragment compounds, which potentially could lead to false positive results (Fig. 4A). Like C99, the spectrum of PMP22 was not perturbed by 4 % D₆-DMSO but showed some significant perturbation at 10 % D₆-DMSO (Fig. 4B). To sum up, the optimized conditions that we found for fragment screening of PMP22 were 150–200 μ M protein in 1.5 or 2 mM DDM micelles (150 mM or 200 mM DDM) with a protein-to-micelle ratio of 1:10 and 4 % D₆-DMSO, and using the b_trotyf3gpqh.2 pulse program with 440 scans in the direct dimension and 96 points in the indirect dimension. Using 200 μ l samples

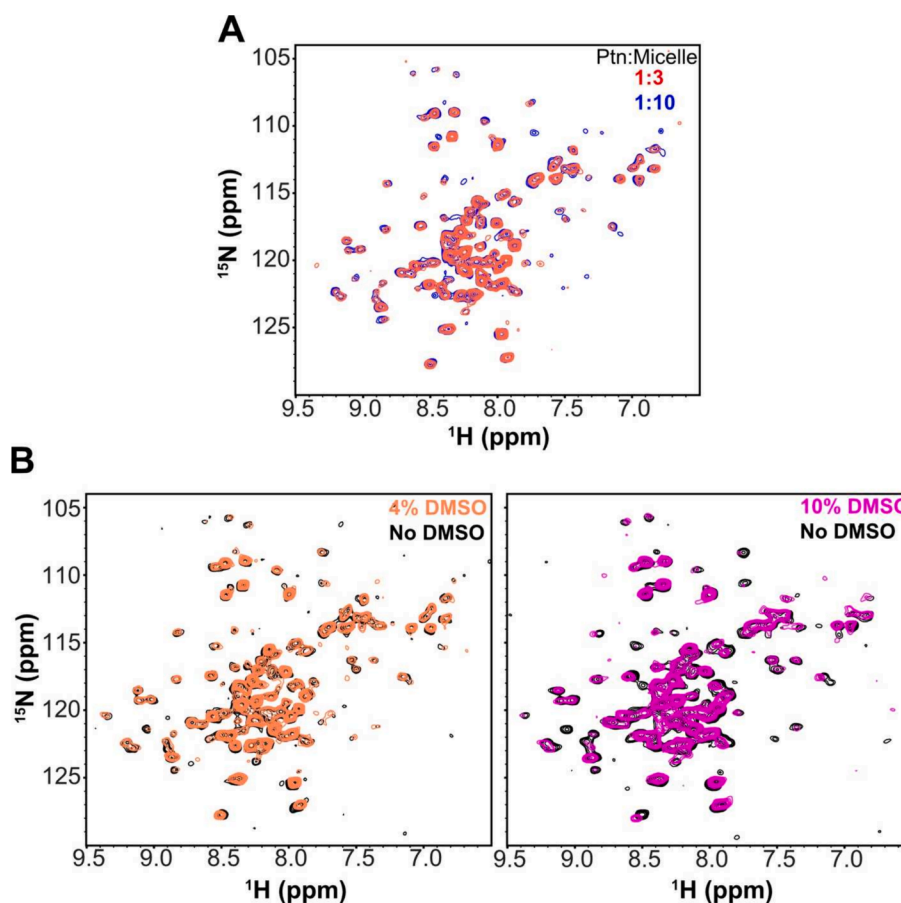


Fig. 4. Optimization of the protein-to-micelle ratio and the D₆-DMSO concentration optimization for screening PMP22. **A)** Overlaid spectra of ¹⁵N-labeled PMP22 at 1:3 and 1:10 protein-to-DDM micelle ratios. The two spectra were very similar to each other. The protein concentration used is 100 μ M while the DDM concentrations are 30 mM (1:3 protein-to-micelle) and 100 mM (1:10 protein-to-micelle). Both experiments were acquired at a sample temperature of 45 °C and 600 MHz. Recycle delay = 0.2 s; number of complex data points: 2048 in the ¹H and 96 in the ¹⁵N dimensions; spectral width: 18 ppm in the ¹H and 28 ppm in the ¹⁵N dimensions. **B)** Overlaid spectra of ¹⁵N-labeled PMP22 in the presence and absence of D₆-DMSO at two different concentrations (4 % and 10 %). The NMR spectrum of PMP22 is largely unperturbed at 4 % D₆-DMSO but showed signs of perturbation at 10 % D₆-DMSO. The protein concentration used is 100 μ M. The experiments were acquired at a sample temperature of 45 °C and 900 MHz. Recycle delay = 0.2 s; number of complex data points: 2048 in the ¹H and 96 in the ¹⁵N dimensions; spectral width: 18 ppm in the ¹H and 28 ppm in the ¹⁵N dimensions.

in 3 mm NMR tubes, the total time required for an experiment at 900 MHz was 4 h.

Examples of results from fragment based screening

Using the optimized conditions, we screened a plate each from the Fesik Fragment Library for C99 and PMP22. Each plate has 96 wells, with each well containing a mixture of 12 fragments at 20 mM each in D₆-DMSO, for a total of 1152 compounds per plate. These mixtures were diluted 25X into the NMR samples (800 μM concentration for each compound). Once a mixture was seen to result in a chemical shift perturbation, it was then further deconvoluted into 4 mixtures of 3 compounds each, and then to individual compounds to identify the hit. For C99, out of the 1152 compounds we screened, we found one hit, VU-MAC-1, that perturbed the chemical shifts of the transmembrane residues A713-L723 (Fig. 5A and B). Interestingly, this compound demonstrated binding in the slow-exchange regime on the NMR timescale. Titration of this compound revealed only a modest apparent K_d value of ~400 μM when the peak volume of the emerging bound-state resonance was monitored during titration (Fig. 5C). The fact that binding is weak

and yet seen to be slow-exchange on the NMR time scale is likely due to the slow rate of diffusion of this compound from empty micelles to C99-containing micelles and vice versa. In this same vein, it is important to note that the K_d obtained from these measurements may not report the true K_d for the on/off binding of the compound to the protein. Since the compounds in the fragment library would generally partition favorably toward the detergent micelles, the measured K_d is really an *apparent* K_d , reflecting two interactions: the affinity of the compound toward the detergent micelles (relative to the aqueous phase) and the affinity of the compound toward the protein in those micelles.

By way of a negative control, we also tested the same compound for non-specific binding against the combined transmembrane and juxtamembrane domains (TM/JM) of the Notch-1 protein under the same conditions (Fig. 5D). Like C99, the Notch-1 TM/JM is also a single-pass transmembrane protein that is a substrate of γ -secretase. We found that while VU-MAC-1 caused a change in the chemical shift of some Notch-1 resonances, they were in the fast-exchange timescale and did not exhibit saturation of binding as the compound was titrated in. This confirms that the interaction between VU-MAC-1 and Notch-1 was much weaker than that between VU-MAC-1 and C99, and most likely non-specific. Finally,

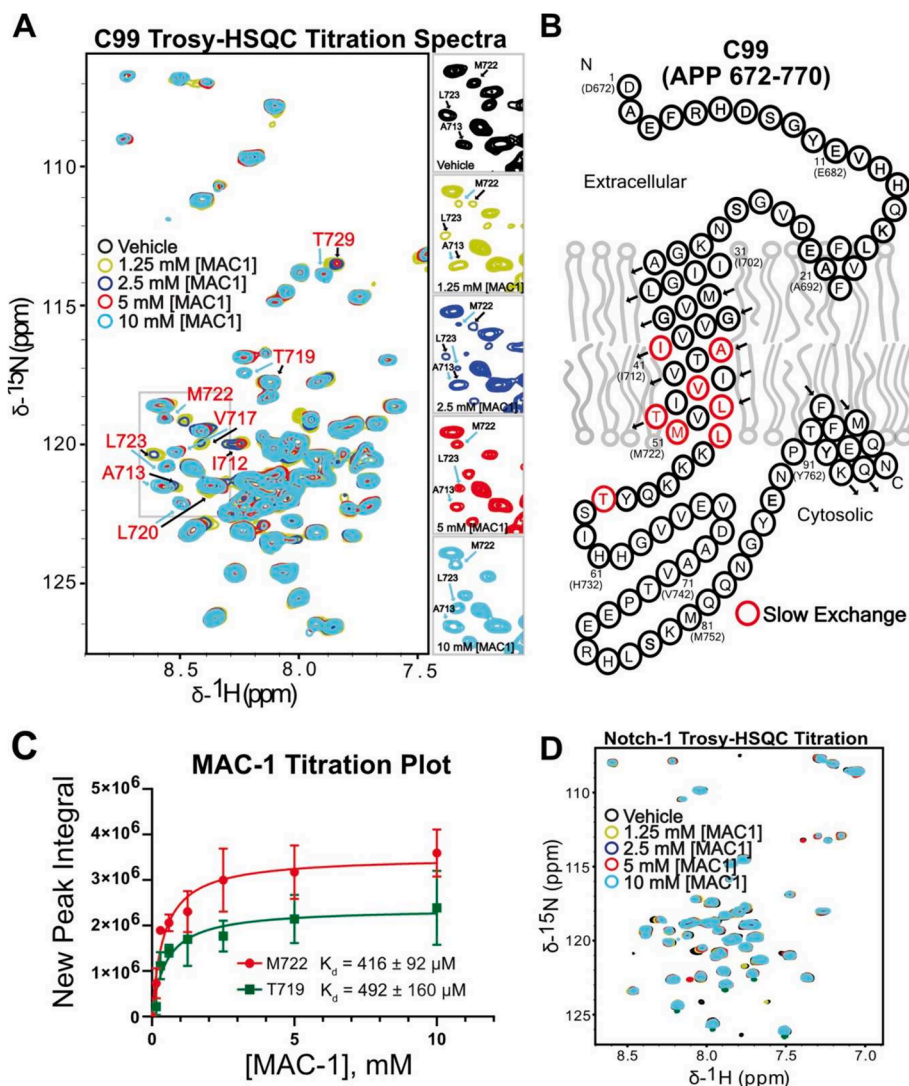


Fig. 5. Initial fragment-based screening results show that VU-MAC-1 specifically associates with C99. A) Five overlaid spectra of U-¹⁵N-C99 at varying VU-MAC-1 concentrations reveal slow exchange peaks upon compound addition. Black and cyan arrows denote the positions of the peak before and after addition of VU-MAC-1, respectively. B) Peaks seen to shift map to the C-terminal transmembrane/juxtamembrane region of the C99 sequence. C) Binding isotherm for the emerging peak intensity representing the C99-bound state as the VU-MAC-1 concentration is increased. D) Notch-1 TM/JM titration with VU-MAC-1 reveals only non-specific, fast-exchange interactions that do not saturate. All experiments were acquired at a sample temperature of 45 °C and 600 MHz.

we note that when VU-MAC-1 was re-ordered from two independent external vendors, the compound was a different color and the results reported here from our in-house library were not reproduced. We believe that VU-MAC-1 is a likely a derivative of the original Fesik library member that formed due to oxidation or hydrolysis during the long (ca. 10 years) storage period for the specific form of this library we used.

Similarly, we also found a Fesik library single hit for PMP22 from the plate we screened. This hit caused chemical shift perturbations in three residues, again in the slow-exchange regime with an apparent K_d of ~ 1 mM (Fig. 6A and B). The compound is VU-GCL-1. We tested this compound with the voltage-sensing domain (VSD) of KCNQ1 in LMPG micelles, which also has four transmembrane helices, like PMP22. We found that this compound did not bind to the voltage-sensing domain of KCNQ1, validating that this compound selectively binds PMP22 (Fig. 6C).

Discussion

This paper describes a protocol for the first stage of fragment-based screening of membrane proteins in detergent micelles by NMR. Building on the SAR-by-NMR approach of Stephen Fesik (Shuker et al., 1996), we extended the first steps of this approach to membrane proteins. Prior to conducting any NMR-based fragment screening of membrane proteins, it is critical to optimize the expression and purification of the membrane protein targets of interest. Here, we chose two human membrane protein

targets: the single pass transmembrane protein C99, and the tetraspan membrane protein PMP22; both of which are associated with diseases. These two proteins have been studied extensively in our lab, such that we have well-established protocols for their expression in *E. coli* and purification. Typical yields for purified C99 and PMP22 are roughly 5 mg and 3.5 mg of purified protein per liter of minimal media, respectively.

The optimal conditions for screening vary depending on the membrane protein target and the membrane mimetic used. In this paper, we show that we have reduced throughput (longer required NMR experimental time even at higher protein concentrations) when targeting a multispan membrane protein than for a single pass membrane protein. However, once a good compromise between spectral quality and experimental time is determined, it is possible to carry out fragment-based screening effectively, with minimal false positive results.

As was the case for both C99 and PMP22, out of the 1152 compounds screened for this methods optimization study, we were able to find one hit per plate, indicating an approximate hit rate of 0.1%. It is likely that false negatives occur in this type of screening. While the Fesik library was carefully designed to remove “bad actors”—compounds that misbehave (Harner et al., 2013), it is possible that some fragments still aggregate, as we observed precipitation in some of our NMR samples. A previous example of this is verteporfin (a compound in an FDA-approved drug library screened in a different study), where we observed aggregation of verteporfin at low LMPG concentrations from NMR and DLS measurements. (Castro et al., 2022) These verteporfin aggregates could

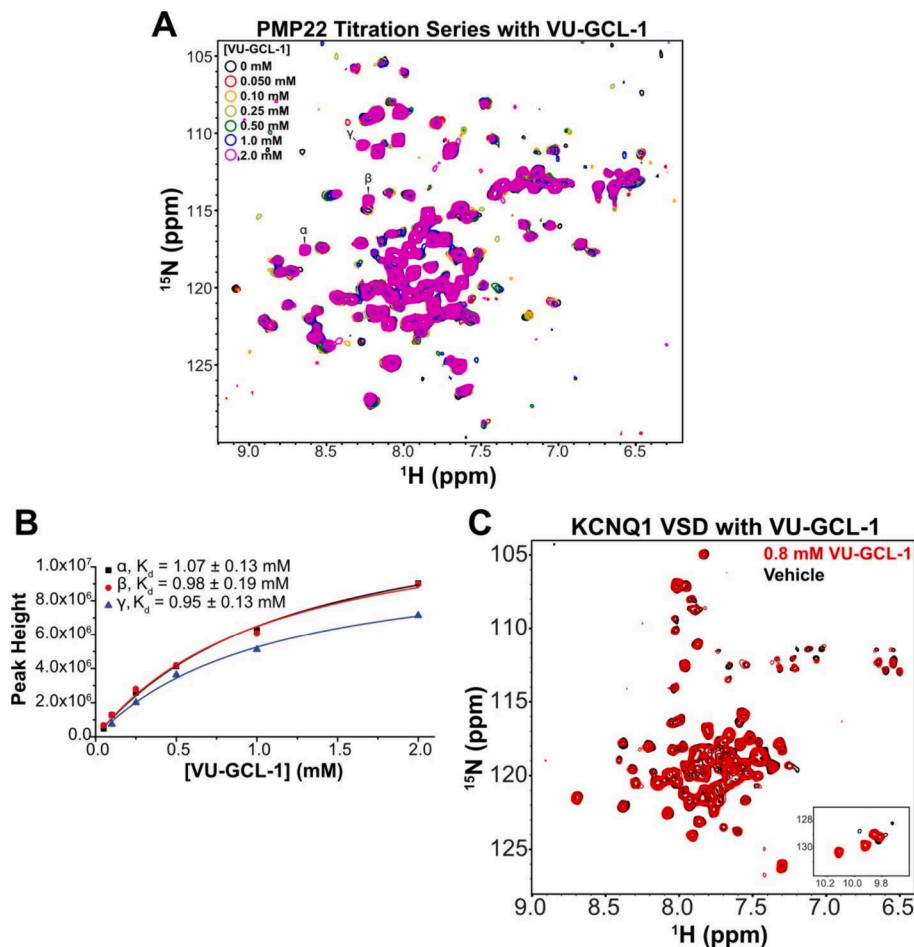


Fig. 6. Initial fragment-based screening results show that VU-GCL-1 binds to PMP22. **A)** Seven overlaid ^{15}N -PMP22 spectra at varying VU-GCL-1 concentrations reveal the appearance of slow exchange peaks upon compound addition (designated by the Greek letters). **B)** Binding isotherm of the emerging peak height of the PMP22-bound state vs. VU-GCL-1 concentration. **C)** Addition of VU-GCL-1 into the voltage-sensing domain (VSD) of KCNQ1 did not show evidence of binding. All experiments were acquired at a sample temperature of 45 °C and 900 MHz.

be dispersed at higher micelle concentrations, mitigating this problem.

In this study, we used protein-to-micelle ratios of 1:16 for C99 and 1:10 for PMP22 to avoid forced cohabitation of protein and fragments that would result in false positive, and also to help prevent compound aggregation of the fragments. Under these conditions, most of the somewhat hydrophobic compounds in the Fesik library will preferentially partition into the detergent micelles relative to the aqueous phase. Fragments can equilibrate between protein-free micelles, protein-containing micelles, and the aqueous phase by direct diffusion of the compounds into and out of micelles to the aqueous phase and also when micelles collide and/or fuse. Because of the low molecular weights of the molecular fragments, even those that are more extremely hydrophobic are still expected to have significant aqueous solubilities (the library was originally developed for screens of water-soluble proteins). Compounds that are seen to bind the membrane protein target do so because it is thermodynamically favored relative to partitioning either into water or into empty micelles. For the proteins and plates used for this study we observed a hit rate of 0.1 %. While this hit rate seems low, we are confident that the hits that we found are true positives as evidenced by the saturation of binding seen in titration plots as well as by apparent lack of interactions with negative control membrane proteins of similar size and membrane topology. These observations echo those made in a previous NMR-based HTS of C99 in micelles with a library of FDA-approved drugs, work in which we discovered that verteporfin is a specific binder of C99 (Castro et al., 2022).

Another consideration is the charge of the detergent used to solubilize the membrane protein target. Charged detergents, such as LMPG, can potentially enhance or diminish the micellar binding affinity of the fragments having ionizable groups. This could potentially alter the hit rate of the screening relative to conditions employing an electroneutral or zwitterionic membrane-mimetic. We note that most of the fragments in the Fesik library are charge-neutral. In general, one has to find the right balance of experimental conditions that produce expeditious and high-quality NMR spectra with an understanding that certain conditions may favor false positives and false negatives. Therefore, it is paramount that rigorous follow-up hit validation be employed, such as testing binding in other membrane mimetics or, as we did, conducting a counterscreen using the same conditions, but a topologically similar negative control protein.

The approach presented here may not be as high throughput as in conventional FBDD using soluble protein targets because of the relatively long time it takes to acquire HSQC or TROSY spectra of membrane proteins. However, it can be envisioned that there are a couple of approaches that may be employed to increase the throughput. One is the more sensitive ¹³C-methyl-TROSY (Tugarinov and Kay, 2004) experiments to look at side-chain methyl groups (Tugarinov and Kay, 2004; Kay, 2011), an approach that may be particularly attractive since membrane proteins have many aliphatic residues in their trans-membrane domains. Also, non-uniform sampling (NUS) methods (Barna et al., 1987; Delaglio et al., 2017) might also be used to decrease the experiment time per sample. Alternatively, one might also explore the use of the newly developed RAPID-TROSY (Manu et al., 2023) pulse sequence, which utilizes an evolutionary algorithm and artificial intelligence in pulse generation. In any case we hope that the NMR-based fragment screening optimization scheme presented in this paper will complement other screening protocols currently used to find small molecule binders to membrane proteins.

Materials and methods

Protein expression and purification

C99 and PMP22 are expressed and purified as described previously by Castro et al. (Castro et al., 2022) and by Stefanski et al. (Stefanski et al., 2023), respectively. Briefly, the human C99 construct has a C-terminal hexa-His-tag and an additional Trp to enhance UV absorption to

facilitate determination of its concentration. This construct was expressed in the *E. coli* BL21(DE3) strain. C99 was then purified in LMPG micelles using Ni(II)-ion affinity chromatography.

PMP22 is expressed as a fusion protein with an N-terminal lambda repressor fragment followed by a deca-His tag, a thrombin cleavage site, and a Strep tag. The fusion protein was expressed in the BL21(DE3)Star strain and then purified in DDM micelles using metal ion affinity chromatography, a process during which the N-terminal fusion protein (except for the Strep tag) was removed by thrombin cleavage.

The negative control proteins, Notch-1 TM/JM and the voltage-sensing domain (VSD) of KCNQ1, were expressed and purified as described previously by Deatherage et al. (Deatherage et al., 2017) and Taylor et al (Taylor et al., 2020), respectively. After purification, the proteins were buffer-exchanged according to their respective NMR buffer conditions (see below) and concentrated with LMPG as the detergent.

Preparation of NMR samples

The final buffer conditions for NMR are as follows:

C99 or Notch-1: 25 mM imidazole or PIPES, 100 mM NaCl, 0.5 mM EDTA, pH 6.5, 2.5 % w/v LMPG, 50 μM protein, 5 % v/v D₂O

PMP22: 20 mM acetate, 100 mM NaCl, 5 mM TCEP, 1 mM EDTA, pH 5.0, 150 or 200 mM DDM, 150 or 200 μM protein, 5 % v/v D₂O

KCNQ1 VSD: 40 mM HEPES, 150 mM NaCl, 2 mM TCEP, pH 7.5, 2 % w/v LMPG, 112 μM protein, 5 % v/v D₂O

The individual protein stock solutions were diluted to their desired concentrations. The final volume of the NMR samples used was 200 μL and they were dispensed into 3 mm x 4 in. NMR tubes fitted with bar-coded caps.

NMR spectroscopy and optimization of screening conditions

The optimization and actual NMR-based screening were conducted using Bruker Avance III 600 MHz or 900 MHz spectrometers equipped with a CPCTI cryoprobe and an automated sample changer (SampleJet). We also set an incubation period of 10 min in between samples to allow them to equilibrate to 318 K before starting the acquisition. NMR spectra were acquired using standard Bruker pulse sequences and at 318 K. All spectra were processed using Bruker TopSpin 3.6 and analyzed using NMR-FAM Sparky.

For optimization of the pulse program for C99 we tested four different pulse programs: troysetf3gpsi.2, sfhmqcf3pph, b_troysetf3gpph.2 and b_troysetf3gpsi.3, as implemented in the Bruker pulse program library. The troysetf3gpsi.2 is the clean-TROSY pulse sequence, proposed by Schulte-Herbrüggen and Sorensen (Schulte-Herbrüggen and Sorensen, 2000), without the S³E filter. The sfhmqcf3gpph is the standard SOFAST HMQC pulse sequence as reported by Schanda et al (Schanda et al., 2005). We used two different versions of BEST-TROSY in the Bruker pulse program library: b_troysetf3gpph.2 and b_troysetf3gpsi.3. They both use the same fundamental BEST-TROSY pulse sequence reported by Favier and Brutscher (Favier and Brutscher, 2011), and both are phase sensitive experiments using Echo/Anti-Echo. The difference between the two pulse programs is that the b_troysetf3gpsi.3 uses shaped pulses for inversion and refocusing on ¹⁵N and enhances sensitivity through the gradient pulses.

Fragment screening

The nearly 14,000-compound fragment library originally developed by Prof. Stephen Fesik was provided by the Vanderbilt High Throughput Screening Core (Harner et al., 2013). The library consists of chemically diverse compounds that are compliant to the rule-of-three (Congreve et al., 2003), with slight modifications, where fragments with molecular weight between 100–250 Da, with up to 4 hydrogen bond donors, and with a ClogP of up to 3.5 were chosen. The library also includes

compounds with chemical groups that are known to bind frequently to proteins such as carboxylic acid-, biphenyl, diphenylmethyl-, and various heterocycles (Hajduk et al., 2000); while removing “bad actors” or compounds that are known to misbehave such as nonspecific binders, covalent modifiers, chelators, and aggregators (Harner et al., 2013).

The compounds are delivered in 96-well plates, where each well contains a mixture of 12 compounds at 20 mM each in D₆-DMSO. Once a mixture was seen to significantly induce chemical shift perturbations in the TROSY spectrum of the target, the mixture was deconvoluted into 4 mixtures of 3 compounds each, and then to individual compounds until the hit(s) causing the changes to the spectrum of the protein target is/are identified. The final concentration of each fragment in the NMR sample during the initial screen was 800 μM. An NMR titration of the hit compound was then conducted by varying concentrations of the hit compound and collecting the TROSY spectrum at each point. The data were then fitted by a 1:1 binding isotherm to determine the apparent K_d.

CRedit authorship contribution statement

Geoffrey C. Li: Writing – original draft, Methodology, Investigation, Formal analysis, Data curation, Conceptualization. **Manuel A. Castro:** Writing – review & editing, Methodology, Investigation, Formal analysis, Data curation, Conceptualization. **Thilini Ukwaththage:** Methodology. **Charles R. Sanders:** Writing – review & editing, Supervision, Funding acquisition, Formal analysis, Conceptualization.

Declaration of competing interest

The authors declare that they have no known competing financial interests or personal relationships that could have appeared to influence the work reported in this paper.

Data availability

Data will be made available on request.

Acknowledgments

We sincerely thank Dr. Stephen Fesik for the use of his fragment library and for advice. We also thank Corbin Whitwell from the Vanderbilt High-throughput Screening core for her essential role in compound distribution and organization of the drug library. We thank Dr. Markus Voehler for his assistance in setting up NMR experiments.

Funding

This work was supported by NIH grants RF1 AG056147 and R01 NS095989, as well as by Deerfield Management Company, L.P. through Ancora Innovation, the Vanderbilt/Deerfield partnership. MAC was supported by the NSF GRFP DGE-1445197 and an NIH predoctoral fellowship F31 AG069462. NMR instrumentation was supported by NSF 0922862, NIH S10 RR025677 and Vanderbilt University matching funds.

References

Barna, J.C.J., Laue, E.D., Mayger, M.R., Skilling, J., Worrall, S.J.P., 1987. Exponential sampling, an alternative method for sampling in two-dimensional nmr experiments. *J. Magn. Reson.* 73 (1), 69–77. [https://doi.org/10.1016/0022-2364\(87\)90225-3](https://doi.org/10.1016/0022-2364(87)90225-3).
 Barrett, P.J., Song, Y., Van Horn, W.D., Hustedt, E.J., Schafer, J.M., Hadziselimovic, A., Beel, A.J., Sanders, C.R., 2012. The amyloid precursor protein has a flexible transmembrane domain and binds cholesterol. *Science* 336 (6085), 1168–1171. <https://doi.org/10.1126/science.1219988>.
 Buchholz, C.R., Pomerantz, W.C.K., 2021. (19)F NMR viewed through two different lenses: ligand-observed and protein-observed (19)F NMR applications for fragment-based drug discovery. *RSC Chem Biol* 2 (5), 1312–1330. <https://doi.org/10.1039/d1cb00085c>.

Carr, R.A., Congreve, M., Murray, C.W., Rees, D.C., 2005. Fragment-based lead discovery: Leads by design. *Drug Discov Today* 10 (14), 987–992. [https://doi.org/10.1016/S1359-6446\(05\)03511-7](https://doi.org/10.1016/S1359-6446(05)03511-7).
 Castro, M.A., Hadziselimovic, A., Sanders, C.R., 2019. The vexing complexity of the amyloidogenic pathway. *Protein Sci* 28 (7), 1177–1193. <https://doi.org/10.1002/pro.3606>.
 Castro, M.A., Parson, K.F., Beg, I., Wilkinson, M.C., Nurmakova, K., Levesque, I., Voehler, M.W., Wolfe, M.S., Ruotolo, B.T., Sanders, C.R., 2022. Verteporfin is a substrate-selective gamma-secretase inhibitor that binds the amyloid precursor protein transmembrane domain. *J Biol Chem* 298 (4), 101792. <https://doi.org/10.1016/j.jbc.2022.101792>.
 Chen, D., Errey, J.C., Heitman, L.H., Marshall, F.H., Ijzerman, A.P., Siegal, G., 2012. Fragment screening of GPCRs using biophysical methods: identification of ligands of the adenosine A(2A) receptor with novel biological activity. *ACS Chem Biol* 7 (12), 2064–2073. <https://doi.org/10.1021/cb300436c>.
 Chow, V.W., Mattson, M.P., Wong, P.C., Gleichmann, M., 2010. An overview of APP processing enzymes and products. *Neuromolecular Med* 12 (1), 1–12. <https://doi.org/10.1007/s12017-009-8104-z>.
 Congreve, M., Carr, R., Murray, C., Jhoti, H., 2003. A ‘rule of three’ for fragment-based lead discovery? *Drug Discov Today* 8 (19), 876–877. [https://doi.org/10.1016/S1359-6446\(03\)02831-9](https://doi.org/10.1016/S1359-6446(03)02831-9).
 Congreve, M., Rich, R.L., Myszkowski, D.G., Figaroa, F., Siegal, G., Marshall, F.H., 2011. Fragment screening of stabilized G-protein-coupled receptors using biophysical methods. *Methods Enzymol* 493, 115–136. <https://doi.org/10.1016/B978-0-12-381274-2.00005-4>.
 Dalvit, C., Peavarello, P., Tato, M., Veronesi, M., Vulpetti, A., Sundstrom, M., 2000. Identification of compounds with binding affinity to proteins via magnetization transfer from bulk water. *J Biomol NMR* 18 (1), 65–68. <https://doi.org/10.1023/a:1008354229396>.
 Dalvit, C., Fogliatto, G., Stewart, A., Veronesi, M., Stockman, B., 2001. WaterLOGSY as a method for primary NMR screening: practical aspects and range of applicability. *J Biomol NMR* 21 (4), 349–359. <https://doi.org/10.1023/a:1013302231549>.
 Dalvit, C., Flocco, M., Veronesi, M., Stockman, B.J., 2002. Fluorine-NMR competition binding experiments for high-throughput screening of large compound mixtures. *Comb Chem High Throughput Screen* 5 (8), 605–611. <https://doi.org/10.2174/1386207023329923>.
 Deatherage, C.L., Lu, Z., Kroncke, B.M., Ma, S., Smith, J.A., Voehler, M.W., McFeeters, R. L., Sanders, C.R., 2017. Structural and biochemical differences between the Notch and the amyloid precursor protein transmembrane domains. *Sci Adv* 3 (4), e1602794.
 Delaglio, F., Walker, G.S., Farley, K.A., Sharma, R., Hoch, J.C., Arboogast, L.W., Brinson, R.G., Marino, J.P., 2017. Non-uniform sampling for all: More NMR spectral quality, less measurement time. *Am Pharm Rev* 20 (4).
 Erlanson, D.A., Fesik, S.W., Hubbard, R.E., Jahnke, W., Jhoti, H., 2016. Twenty years on: The impact of fragments on drug discovery. *Nat Rev Drug Discov* 15 (9), 605–619. <https://doi.org/10.1038/nrd.2016.109>.
 Erlanson, D.A., Hansen, S.K., 2004. Making drugs on proteins: site-directed ligand discovery for fragment-based lead assembly. *Curr Opin Chem Biol* 8 (4), 399–406. <https://doi.org/10.1016/j.cbpa.2004.06.010>.
 Favier, A., Brutscher, B., 2011. Recovering lost magnetization: polarization enhancement in biomolecular NMR. *J Biomol NMR* 49 (1), 9–15. <https://doi.org/10.1007/s10858-010-9461-5>.
 Fejzo, J., Lepre, C., Xie, X., 2003. Application of NMR screening in drug discovery. *Curr Top Med Chem* 3 (1), 81–97. <https://doi.org/10.2174/1568026033392796>.
 Fesik, S.W., Shuker, S.B., Hajduk, P.J., Meadows, R.P., 1997. SAR by NMR: An NMR-based approach for drug discovery. *Protein Eng* 10, 73.
 Fruh, V., Zhou, Y., Chen, D., Loch, C., Ab, E., Grinkova, Y.N., Verheij, H., Sligar, S.G., Bushweller, J.H., Siegal, G., 2010. Application of fragment-based drug discovery to membrane proteins: identification of ligands of the integral membrane enzyme DsbB. *Chem Biol* 17 (8), 881–891. <https://doi.org/10.1016/j.chembiol.2010.06.011>.
 Hajduk, P.J., Meadows, R.P., Fesik, S.W., 1999. NMR-based screening in drug discovery. *Q Rev Biophys* 32 (3), 211–240. <https://doi.org/10.1017/s0033583500003528>.
 Hajduk, P.J., Gerfin, T., Boehlen, J.M., Haberli, M., Marek, D., Fesik, S.W., 1999. High-throughput nuclear magnetic resonance-based screening. *J Med Chem* 42 (13), 2315–2317. <https://doi.org/10.1021/jm9901475>.
 Hajduk, P.J., Bures, M., Praetgaard, J., Fesik, S.W., 2000. Privileged molecules for protein binding identified from NMR-based screening. *J Med Chem* 43 (18), 3443–3447. <https://doi.org/10.1021/jm00164q> From NLM Medline.
 Hajduk, P.J., Greer, J., 2007. A decade of fragment-based drug design: strategic advances and lessons learned. *Nat Rev Drug Discov* 6 (3), 211–219. <https://doi.org/10.1038/nrd2220>.
 Harner, M.J., Frank, A.O., Fesik, S.W., 2013. Fragment-based drug discovery using NMR spectroscopy. *J Biomol NMR* 56 (2), 65–75. <https://doi.org/10.1007/s10858-013-9740-z> From NLM Medline.
 Homans, S.W., 2004. NMR spectroscopy tools for structure-aided drug design. *Angew Chem Int Ed Engl* 43 (3), 290–300. <https://doi.org/10.1002/anie.200300581>.
 Igonet, S., Raingeval, C., Cecon, E., Pucic-Bakovic, M., Lauc, G., Cala, O., Baranowski, M., Perez, J., Jockers, R., Krimm, I., Jawhari, A., 2018. Enabling STD-NMR fragment screening using stabilized native GPCR: A case study of adenosine receptor. *Sci Rep* 8 (1), 8142. <https://doi.org/10.1038/s41598-018-26113-0>.
 Jetten, A.M., Suter, U., 2000. The peripheral myelin protein 22 and epithelial membrane protein family. *Prog Nucleic Acid Res Mol Biol* 64, 97–129. [https://doi.org/10.1016/S0079-6603\(00\)64003-5](https://doi.org/10.1016/S0079-6603(00)64003-5).
 Jordan, J.B., Poppe, L., Xia, X., Cheng, A.C., Sun, Y., Michelsen, K., Eastwood, H., Schnier, P.D., Nixey, T., Zhong, W., 2012. Fragment based drug discovery: practical

- implementation based on (1)(9)F NMR spectroscopy. *J Med Chem* 55 (2), 678–687. <https://doi.org/10.1021/jm201441k>.
- Kay, L.E., 2011. Solution NMR spectroscopy of supra-molecular systems, why bother? A methyl-TROSY view. *J Magn Reson* 210 (2), 159–170. <https://doi.org/10.1016/j.jmr.2011.03.008>.
- Lambruschini, C., Veronesi, M., Romeo, E., Garau, G., Bandiera, T., Piomelli, D., Scarpelli, R., Dalvit, C., 2013. Development of fragment-based n-FABS NMR screening applied to the membrane enzyme FAAH. *Chembiochem* 14 (13), 1611–1619. <https://doi.org/10.1002/cbic.201300347>.
- Li, J., Parker, B., Martyn, C., Natarajan, C., Guo, J., 2013. The PMP22 gene and its related diseases. *Mol Neurobiol* 47 (2), 673–698. <https://doi.org/10.1007/s12035-012-8370-x>.
- Manu, V.S., Olivieri, C., Veglia, G., 2023. AI-designed NMR spectroscopy RF pulses for fast acquisition at high and ultra-high magnetic fields. *Nat Commun* 14 (1). <https://doi.org/10.1038/s41467-023-39581-4>.
- Mayer, M., Meyer, B., 1999. Characterization of ligand binding by saturation transfer difference NMR spectroscopy. *Angew Chem Int Ed Engl* 38 (12), 1784–1788. [https://doi.org/10.1002/\(SICI\)1521-3773\(19990614\)38:12<1784::AID-ANIE1784>3.0.CO;2-Q](https://doi.org/10.1002/(SICI)1521-3773(19990614)38:12<1784::AID-ANIE1784>3.0.CO;2-Q).
- Mayer, M., Meyer, B., 2001. Group epitope mapping by saturation transfer difference NMR to identify segments of a ligand in direct contact with a protein receptor. *J Am Chem Soc* 123 (25), 6108–6117. <https://doi.org/10.1021/ja0100120>.
- Meinecke, R., Meyer, B., 2001. Determination of the binding specificity of an integral membrane protein by saturation transfer difference NMR: RGD peptide ligands binding to integrin alphaIIb beta3. *J Med Chem* 44 (19), 3059–3065. <https://doi.org/10.1021/jm0109154>.
- Mureddu, L.G., Vuister, G.W., 2022. Fragment-based drug discovery by NMR. Where are the successes and where can it be improved? *Front Mol Biosci* 9, 834453. <https://doi.org/10.3389/fmolb.2022.834453>.
- Murray, C.W., Rees, D.C., 2009. The rise of fragment-based drug discovery. *Nat Chem* 1 (3), 187–192. <https://doi.org/10.1038/nchem.217>.
- Murray, C.W., Verdonk, M.L., Rees, D.C., 2012. Experiences in fragment-based drug discovery. *Trends Pharmacol Sci* 33 (5), 224–232. <https://doi.org/10.1016/j.tips.2012.02.006>.
- Norton, R.S., Leung, E.W., Chandrashekar, I.R., MacRaid, C.A., 2016. Applications of (19)F-NMR in fragment-based drug discovery. *Molecules* 21 (7). <https://doi.org/10.3390/molecules21070860>.
- Oliver, R.C., Lipfert, J., Fox, D.A., Lo, R.H., Doniach, S., Columbus, L., 2013. Dependence of micelle size and shape on detergent alkyl chain length and head group. *PLoS One* 8 (5), e62488.
- Opella, S.J., Kim, Y., McDonnell, P., 1994. Experimental nuclear magnetic resonance studies of membrane proteins. *Methods Enzymol* 239, 536–560. [https://doi.org/10.1016/s0076-6879\(94\)39021-5](https://doi.org/10.1016/s0076-6879(94)39021-5).
- Pervushin, K., Riek, R., Wider, G., Wuthrich, K., 1997. Attenuated T2 relaxation by mutual cancellation of dipole-dipole coupling and chemical shift anisotropy indicates an avenue to NMR structures of very large biological macromolecules in solution. *Proc Natl Acad Sci U S A* 94 (23), 12366–12371. <https://doi.org/10.1073/pnas.94.23.12366>.
- Rees, D.C., Congreve, M., Murray, C.W., Carr, R., 2004. Fragment-based lead discovery. *Nat Rev Drug Discov* 3 (8), 660–672. <https://doi.org/10.1038/nrd1467>.
- Schanda, P., Kupce, E., Brutscher, B., 2005. SOFAST-HMQC experiments for recording two-dimensional heteronuclear correlation spectra of proteins within a few seconds. *J Biomol NMR* 33 (4), 199–211. <https://doi.org/10.1007/s10858-005-4425-x>.
- Schulte-Herbruggen, T., Sorensen, O.W., 2000. Clean TROSY: compensation for relaxation-induced artifacts. *J Magn Reson* 144 (1), 123–128. <https://doi.org/10.1006/jmre.2000.2020> From NLM Medline.
- Shuker, S.B., Hajduk, P.J., Meadows, R.P., Fesik, S.W., 1996. Discovering high-affinity ligands for proteins: SAR by NMR. *Science* 274 (5292), 1531–1534. <https://doi.org/10.1126/science.274.5292.1531>.
- Stefanski, K.M., Li, G.C., Marinko, J.T., Carter, B.D., Samuels, D.C., Sanders, C.R., 2023. How T118M peripheral myelin protein 22 predisposes humans to Charcot-Marie-Tooth disease. *J Biol Chem* 299 (2), 102839. <https://doi.org/10.1016/j.jbc.2022.102839>.
- Taylor, K.C., Kang, P.W., Hou, P., Yang, N.D., Kuenze, G., Smith, J.A., Shi, J., Huang, H., White, K.M., Peng, D., et al., 2020. Structure and physiological function of the human KCNQ1 channel voltage sensor intermediate state. *Elife* 9. <https://doi.org/10.7554/eLife.53901>.
- Tengel, T., Fex, T., Emtenas, H., Almqvist, F., Sethson, I., Kihlberg, J., 2004. Use of 19F NMR spectroscopy to screen chemical libraries for ligands that bind to proteins. *Org Biomol Chem* 2 (5), 725–731. <https://doi.org/10.1039/b313166a>.
- Tugarinov, V., Kay, L.E., 2004. An isotope labeling strategy for methyl TROSY spectroscopy. *J Biomol NMR* 28 (2), 165–172. <https://doi.org/10.1023/B:JNMR.0000013824.93994.1f>.
- Vanwetswinkel, S., Heetebrij, R.J., van Duynhoven, J., Hollander, J.G., Filippov, D.V., Hajduk, P.J., Siegal, G., 2005. TINS, target immobilized NMR screening: an efficient and sensitive method for ligand discovery. *Chem Biol* 12 (2), 207–216. <https://doi.org/10.1016/j.chembiol.2004.12.004>.
- Viegas, A., Manso, J., Nobrega, F.L., Cabrita, E.J., 2011. Saturation-transfer difference (STD) NMR: A simple and fast method for ligand screening and characterization of protein binding. *J Chem Educ* 88 (7), 990–994. <https://doi.org/10.1021/ed101169t>.
- Vinogradova, O., Sonnichsen, F., Sanders, C.R., 1998. 2nd. On choosing a detergent for solution NMR studies of membrane proteins. *J Biomol NMR*. 11 (4), 381–386. <https://doi.org/10.1023/a:1008289624496> From NLM Medline.
- Zhuang, T., Jap, B.K., Sanders, C.R., 2011. Solution NMR approaches for establishing specificity of weak heterodimerization of membrane proteins. *J Am Chem Soc* 133 (50), 20571–20580. <https://doi.org/10.1021/ja208972h>.